Cerebral Cortex, January 2017;27: 173–184

doi: 10.1093/cercor/bhw335
Advance Access Publication Date: 5 December 2016
Original Article

ORIGINAL ARTICLE

Structural Pathways Supporting Swift Acquisition of New Visuomotor Skills

Ari E. Kahn[1,2,3], Marcelo G. Mattar[4], Jean M. Vettel[2,3,5], Nicholas F. Wymbs[6], Scott T. Grafton[5], and Danielle S. Bassett[2,7]

[1]Department of Neuroscience, University of Pennsylvania, Philadelphia, PA 19104, USA, [2]Department of Bioengineering, University of Pennsylvania, Philadelphia, PA 19104, USA, [3]Human Research and Engineering Directorate, U.S. Army Research Laboratory, Aberdeen, MD 21001, USA, [4]Department of Psychology, University of Pennsylvania, Philadelphia, PA 19104, USA, [5]Department of Psychological and Brain Sciences, University of California, Santa Barbara, CA 93106, USA, [6]Department of Physical Medicine and Rehabilitation, Johns Hopkins University, Baltimore, MD 21218, USA, and [7]Department of Electrical and Systems Engineering, University of Pennsylvania, Philadelphia, PA 19104, USA

Address correspondence to Danielle S. Bassett. Email: dsb@seas.upenn.edu.

Abstract

Human skill learning requires fine-scale coordination of distributed networks of brain regions linked by white matter tracts to allow for effective information transmission. Yet how individual differences in these anatomical pathways may impact individual differences in learning remains far from understood. Here, we test the hypothesis that individual differences in structural organization of networks supporting task performance predict individual differences in the rate at which humans learn a visuomotor skill. Over the course of 6 weeks, 20 healthy adult subjects practiced a discrete sequence production task, learning a sequence of finger movements based on discrete visual cues. We collected structural imaging data, and using deterministic tractography generated structural networks for each participant to identify streamlines connecting cortical and subcortical brain regions. We observed that increased white matter connectivity linking early visual regions was associated with a faster learning rate. Moreover, the strength of multiedge paths between motor and visual modules was also correlated with learning rate, supporting the potential role of extended sets of polysynaptic connections in successful skill acquisition. Our results demonstrate that estimates of anatomical connectivity from white matter microstructure can be used to predict future individual differences in the capacity to learn a new motor–visual skill, and that these predictions are supported both by direct connectivity in visual cortex and indirect connectivity between visual cortex and motor cortex.

Key words: diffusion MRI, discrete sequence production, graph theory, motor sequence learning, polysynaptic networks

Introduction

Human skill learning is a complex phenomenon that involves the fine-scale coordination of disparate cortical and subcortical regions (Dayan and Cohen 2011). This coordination critically depends on the effective transmission of information across white matter tracts, which link distant brain regions in cortico-cortical networks and cortico-subcortical loops (Lynch and Tian 2006). Lesions or injuries to these interconnected tracts—particularly in motor and visual systems—can directly cause deficits in skill learning (Ding et al. 2001). The exact extent of

these deficits is difficult to predict, largely due to the fact that white matter tracts form a complex interconnected network (Sporns et al. 2005). Damage to this network can have broadly distributed repercussions on processing, causing loss of information transmission (Scantlebury et al. 2014), or detrimental alterations in transmission patterns (Crofts et al. 2011).

The interconnected nature of white matter tracts not only complicates response to injury but it also forms a fundamental substrate for individual differences in brain anatomy that may have nontrivial effects on cognition and behavior. White matter connectivity displays large-scale differences across individuals (Bassett et al. 2011), being modulated by age (Betzel et al. 2014), gender (Ingalhalikar et al. 2014, Tunc et al. 2016), genetics (Hong et al. 2015), and prior experience (Scholz et al. 2009, Sampaio-Baptista et al. 2013). How these individual differences may account for individual differences in skill learning is not fully understood. Gaining such an understanding could directly inform therapeutic interventions to enhance recovery of motor skills after brain injury (Tomassini et al. 2011), and furthermore could potentially inform training paradigms to enhance motor–visual expertise in healthy individuals (Neumann et al. 2016).

Here, we examine if connectivity networks defined by diffusion magnetic resonance imaging (MRI) are predictive of individual differences in the rate at which subjects acquire a simple visuomotor task (Wymbs and Grafton 2015). In a discrete sequence production (DSP) task, subjects perform a sequence of finger movements based on visual cues (Rhodes et al. 2004). Once the correct key for each movement is pressed, the visual cue for the next sequence element is presented without delay. Consequently, a DSP task allows subjects to develop exceptionally fast, contiguous movements, much like an expert pianist performing a keyboard arpeggio. Efficient acquisition of this specific visuomotor skill requires a gradual autonomy of visual and motor functional subnetworks (Bassett et al. 2013, 2015) (Fig. 1A, B). Initially, a person relies on the visual cue to perform a finger movement, an action that requires integration between motor and visual cortices; however, once a sequence becomes overlearned, a subject has mastered direct motor–motor associations where a given finger movement is the cue for the next finger movement.

These functional network changes may depend on underlying structure, shown to be a fundamental driver of brain dynamics at rest (Honey et al. 2009, Becker et al. 2015, Goni et al. 2014) and during task performance (Smith et al. 2009, Hermundstad et al. 2013, 2014, Jarbo and Verstynen 2015, Osher et al. 2016). Furthermore, individual variability in behavior has been linked to differences in structural networks (Johansen-Berg 2010), and IQ and motor speed have been associated with greater white matter connectivity (Li et al. 2009) and fractional anisotropy (FA) (Hirsiger et al. 2016). Prior work in word learning tasks also suggests that increased myelination, axonal diameter, and FA in tracts implicated in task processing are associated with better performance (Wong et al. 2011, Lopez-Barroso et al. 2013). Building on these prior studies, we hypothesized that individuals with greater structural connectivity in motor and visual cortices (and particularly in primary motor and visual cortices) would show faster learning rates than individuals with less connectivity. We also set out to test whether these structural differences remained constant over the 6 weeks of practice (Le Bihan and Johansen-Berg 2012) or changed appreciably with training (Scholz et al. 2009, Blumenfeld-Katzir et al. 2011, Taubert et al. 2012). Finally, due to the prevalence of physically extended sets of polysynaptic connections in the visual–motor system, we hypothesized that individual differences in long-distance walks on the graph of structural connections between visual and motor cortex would correspond to individual differences in learning rate.

To address these hypotheses, we examined diffusion tensor imaging (DTI) data acquired from 20 healthy young adult subjects over the course of 6 weeks of training on the DSP task (Bassett et al. 2013, 2014, 2015, Wymbs and Grafton 2015). Subjects were scanned in 4 separate sessions, including a scan on Day 1 before training began and then a scan approximately every 2 weeks. Between scanning sessions, subjects practiced a set of 10-element sequences at home using a program installed on their laptop computers, and behavioral performance was assessed by calculating the movement time (MT) for each sequence defined as the duration between the first button press and the last button press in the sequence. The learning rate for each participant was computed as the first exponential drop-off parameter in a double-exponential fit of the MT as a function of trials practiced across the entire 6 weeks of training. To compare individual differences in learning rate to the organization of white matter connectivity, we generated structural networks from the 4 DTI scans using a deterministic fiber tracking algorithm (Fig. 1C), which provided estimates of the number of streamlines connecting pairs of cortical and subcortical regions derived from brain atlases (Fig. 1D). We observe 3 main results: individual differences in learning rate are significantly correlated with white matter connectivity in visual (but not motor) cortex, these relationships are consistent across the 6 weeks of task practice, and individuals with faster learning rates also show greater *walk strength* linking motor and visual cortices, a measure suggesting increased strength of polysynaptic pathways.

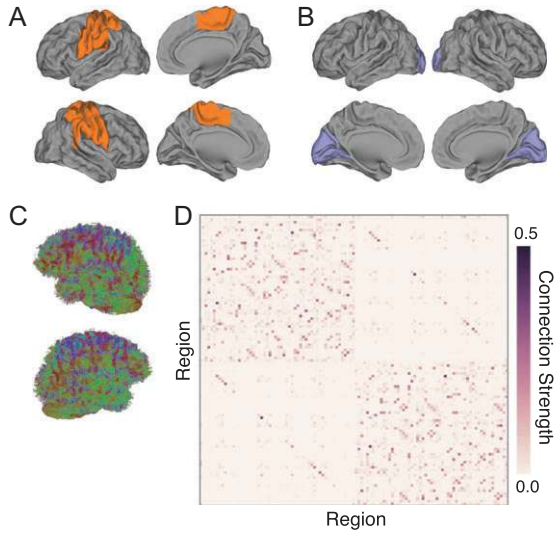

Figure 1. Structural connectivity in motor and visual networks of interest. (*A*, *B*) Previous research suggests that increased skill on the DSP task requires concerted functional network changes in distributed regions of motor (*A*) and visual (*B*) systems (Bassett et al. 2015, 2013); see Table 2 for region names. (*C*) To assess structural correlates of individual differences in learning rate on the DSP task, we performed deterministic diffusion imaging tractography on 4 scans dispersed evenly throughout the 6 weeks of training. (*D*) We constructed structural networks using diffusion imaging tractography and the 111 cortical and subcortical regions in the Harvard-Oxford atlas to examine individual variability in connectivity strength. We also show that our results are robust across atlases, replicating our findings in the 90 cortical and subcortical regions parcellation of the AAL atlas.

Materials and Methods

Participants and Experimental Design

Participants: Twenty-two right-handed participants (13 females and 9 males; mean age, 24 years) volunteered and provided informed consent in writing in accordance with the guidelines of the Institutional Review Board of the University of California, Santa Barbara. All had normal or corrected vision and no history of neurological disease or psychiatric disorders. We excluded 2 participants because 1 participant failed to complete the experiment and the other had excessive head motion (persistent head motion greater than 5 mm during the MRI scanning). We also had technical problems for 2 participants and were unable to collect DTI data during the pretraining session for Scan 1. Finally, for one additional subject, Scan 1 was removed due to the total of estimated streamlines differing by more than 3 standard deviations from the subject mean. Therefore, the structural analysis includes 17 participants for Scan 1 and 20 participants for Scans 2–4.

Experimental setup and procedure: The DSP training protocol occurred over a 6-week period with 4 MRI scanning sessions spaced 2 weeks apart on Day 1, Day 14, Day 28, and Day 42 (Fig. 2A). On Day 1 of the experimental protocol, the participants completed their first MRI session, Scan 1, and the experimenter (N.F.W.) installed the training module on the participant's personal laptop and taught them how to use it for at-home training sessions. Participants were required to do the training for a minimum of 10 out of the 14 days in each 2-week period between the subsequent scanning sessions for Scans 2–4. All participants completed the full expected training regimen; none completed less than 10 full training sessions.

In their at-home training sessions, participants practiced a set of 10-element sequences using their right hand in a DSP task (Bassett et al. 2013, 2014, 2015, Mattar et al. 2015, Wymbs and Grafton 2015). Sequences were presented using a horizontal array of 5 square stimuli, and the key responses were mapped from left to right, such that the thumb corresponded to the leftmost stimulus and the pinky finger corresponded to the rightmost stimulus (Fig. 2B). A square highlighted in red served as the imperative stimulus, and the next square in the sequence was highlighted immediately after each correct key press. If an incorrect key was pressed, the sequence was paused at the error and restarted upon the appropriate key press. Participants had an unlimited amount of time to respond and complete each trial.

Each practice trial began with the presentation of a sequence-identity cue that identified 1 of 6 sequences. These 6 sequences were presented with 3 different levels of exposure, in order to acquire data over a larger range of learning stages while controlling for the effect of scanning day (Table 1). The 2 extensively trained (EXT) sequences were identified with a colored circle (cyan for sequence A and magenta for B), and they were each practiced for 64 trials during every at-home training session. The 2 moderately trained (MOD) sequences were identified by triangles (red for sequence C and green for D) and each practiced for 10 trials in every session. The 2 minimally trained (MIN) sequences were identified by black outlined stars (filled with orange for sequence E and white for F) and only practiced for 1 trial each during the at-home training sessions. Participants were given feedback every 10 trials that reported the number of error-free sequences and the mean time required to complete them.

During each of the 4 MRI scanning sessions, we collected functional echo planar imaging data and structural imaging data from magnetization prepared rapid acquisition gradient-echo (MPRAGE) and DTI scans. In the functional runs, participants performed 300 trials of the self-paced DSP task using the same block structure with feedback as the at-home practice sessions, but the sequences were presented equally for a total of 50 trials for each of the 6 trained sequences. We have previously reported results from functional analyses (Bassett et al. 2013, 2014, 2015, Mattar et al. 2015, Wymbs and Grafton 2015). In this paper, we analyze the structural data and examine individual variability in structural connections among the distributed motor and visual regions of interest that were derived directly from the functional neuroimaging studies of this same data set (Bassett et al. 2015). In this previous work, a set of motor and visual regions that formed functional modules was identified in a data-driven fashion whose task-based modulation tracked the effects of training. Here we build on the identification of these regions of interest by studying their structural connectivity derived from diffusion imaging.

Table 1 Number of trials practiced of each sequence type at the start of each scanning session

	Scan 1	Scan 2	Scan 3	Scan 4
MIN sequences	50	110	170	230
MOD sequences	50	200	350	500
EXT sequences	50	740	1430	2120

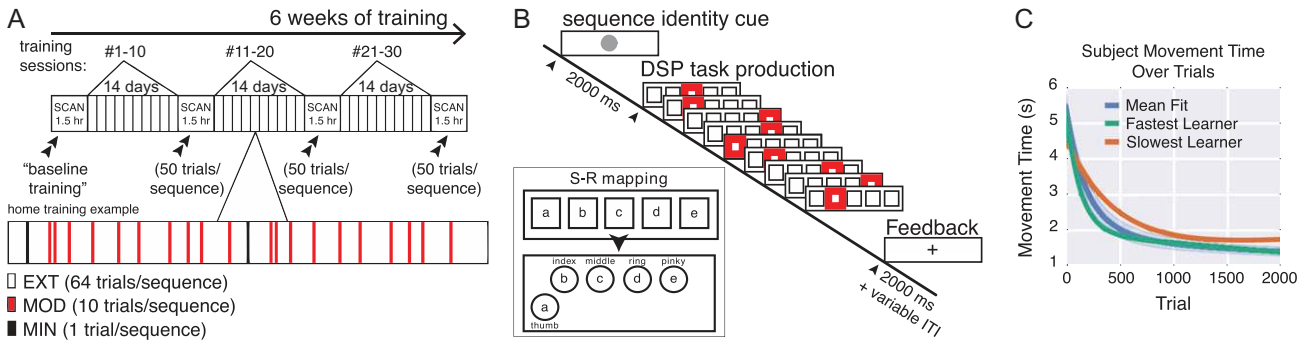

Figure 2. Overview of training, task paradigm, and MT estimation. (*A*) Training schedule. Subjects underwent 4 scans, each approximately 2 weeks apart. Subjects practiced once a day for at least 10 days between each scanning session. (*B*) Subjects viewed a screen on which stimuli were displayed. Each sequence was preceded with the display of a sequence-identity cue, which informed the subject which of 6 sequences would follow. During the sequence, subjects saw 5 horizontally arranged squares. For each element of the sequence, one box was highlighted for the subject, providing information on the key to press. Upon completion of the task, a fixation cross was displayed for a short inter-trial interval, and every 10 trials performance feedback was provided. The squares were spatially mapped onto a keypad, one corresponding to each finger in addition to the thumb (see insert). (*C*) Double-exponential fit of MT to the number of trials practiced. The fit is shown for the fastest learner, the slowest learner, and the mean across all subjects.

Estimating Learning Rates for Individual Participants

For each sequence, we defined the MT as the duration between the time of the first button press and the time of the last button press. For the set of sequences of a single type (i.e., sequence A, B, C, D, E, and F), we estimated the learning rate by fitting a double-exponential function to the MT data (Schmidt and Lee 2005, Rosenbaum 2014) using a robust outlier correction in MATLAB (using the function "fit.m" in the Curve Fitting Toolbox with option "Robust" and type "Lar"): $MT = D_1 e^{-t\kappa} + D_2 e^{-t\lambda}$, where t is time, κ is the exponential drop-off parameter (which we called the *learning rate*) used to describe the fast rate of improvement, λ is the exponential drop-off parameter used to describe the slow, sustained rate of improvement, and D_1 and D_2 are real and positive constants. The magnitude of κ indicates the steepness of the learning slope: individuals with larger κ values have a steeper drop-off in MT, suggesting that they are faster learners (Yarrow et al. 2009, Dayan and Cohen 2011). The decrease in MT has been used to quantify learning for several decades (Snoddy 1926, Crossman 2010). Several functional forms have been suggested for the fit of MT (Newell and Rosenbloom 1993, Heathcote et al. 2000), and variants of an exponential are viewed as the most statistically robust choices (Heathcote et al. 2000). In addition, the fitting approach that we used has the advantage of estimating the rate of learning independent of initial performance or performance ceiling. For the purpose of measuring effects on learning rate, we used the average value of κ for the 2 extensively trained sequences, for which we had the greatest number of trials practiced (Table 1).

While we do not have explicit information on the computing power of each subject's laptop, the learning rate that we study is independent of the starting MT, the ending MT, and the mean MT. Instead, it is a measure of the rate of change in MT. Thus, any differences in computing power cannot be used to explain the results. Moreover, we should mention that error rates on this task are on the order of 1×10^{-3} (Bassett et al. 2015), and error rates are not significantly correlated with learning rates ($r = 0.34$, $p = 0.13$) (Bassett et al. 2015).

Neuroanatomical Data and Associated Methods

In this section, we briefly describe the neuroanatomical data acquired from participants, as well as computational methods associated with data preprocessing, structural network construction, and statistical analyses.

Data Acquisition

All scans were acquired on a 3T Siemens TIM Trio scanner with a 12-channel phased-array head coil at the University of California, Santa Barbara. Each data acquisition session included both a DTI scan as well as a high-resolution T1-weighted anatomical scan. The structural scan was conducted with an echo planar diffusion weighted technique acquired with iPAT using an acceleration factor of 2. The diffusion scan was 30-directional with a b value of 1000 s/mm^2 and TE/TR = 94/8400 ms, in addition to 2 b0 images. Matrix size was 128 × 128 with a slice number of 60. Field of view was 230 × 230 mm^2 and slice thickness was 2 mm. Acquisition time per DTI scan was 9:09 min. The anatomical scan was a high-resolution 3D T1-weighted sagittal whole-brain image using an MPRAGE sequence. It was acquired with TR = 2300 ms; TE = 2.98 ms; flip angle = 9 degrees; 160 slices; 1.10 mm thickness.

DTI Preprocessing

DTI is both highly sensitive to subject movement (Yendiki et al. 2013) and susceptible to directional eddy currents, which can cause distortions in the brain volume (Jezzard et al. 1998). To address these issues, we performed the following data preprocessing using the FMRIB Software Library (FSL v5.0.8) (Smith et al. 2004, Jenkinson et al. 2012). First, individual subject masks of the brain were created with the brain extraction tool (Smith 2002) for use in later registration and correction tools, which require an accurate estimation of the spatial extent of the brain. We applied the EDDY correction tool (Andersson and Sotiropoulos 2016) which simultaneously models both motion effects and eddy current distortions, and corrects them relative to a $b = 0$ image collected at the beginning of the scan.

Next, subject scans were transformed into a common space to compare regional connectivity between subjects. Using FMRIB's linear image registration tool (Jenkinson and Smith 2001, Jenkinson et al. 2002), scans were registered to the anatomical T1 image, and then the anatomical scan was in turn registered to the Montreal Neurological Institute (MNI) space MNI152 template using FMRIB's nonlinear image registration tool (FNIRT). Motion correction also impacts the effective b-matrix directions since the rotated images are no longer aligned with the scanner; therefore, we used the output of EDDY to rotate the b-vectors to match the changes induced by the motion correction procedure (Leemans and Jones 2009).

Using DSI-Studio (http://dsi-studio.labsolver.org), orientation density functions (ODFs) within each voxel were reconstructed from the corrected scans in native diffusion space in order to minimize sampling distortions (Cieslak and Grafton 2014). We then used the reconstructed ODFs to perform a whole-brain deterministic tractography using DSI-Studio (Yeh et al. 2013). We generated 1,000,000 streamlines per subject, with a maximum turning angle of 35 degrees (Bassett et al. 2011) and a maximum length of 500 mm (Cieslak and Grafton 2014). By holding the number of streamlines between participants constant, we use the number of streamlines that connect brain region pairs as an estimate of the strength of the connection and examine individual variability in structural connectivity (Griffa et al. 2013).

Network Construction

To examine the relationship between structural connectivity and individual differences in learning rate, we constructed networks for each subject where nodes are atlas regions and edges are the measured connection strength between region pairs (Hagmann et al. 2008).

The nodes of the network were derived from spatially defined regions of a brain atlas, and we utilized 2 complementary atlas parcellations to confirm that our results are not specific to the particular regional boundaries chosen by one atlas. First, we used the Harvard-Oxford atlas to allow for direct comparison to functional network studies of this same task (Bassett et al. 2013, 2014, 2015), and we combined the Harvard-Oxford cortical and subcortical atlases into a single 111-region atlas by giving cortical labels precedence whenever a single voxel was assigned to both cortical and subcortical regions. In our intrahemisphere vs interhemisphere analysis, we exclude the brainstem region from this atlas since it crosses the midline. As a complementary parcellation, we chose the anatomically defined automated anatomical labeling (AAL) atlas, originally developed in statistical parametric mapping (Tzourio-Mazoyer et al. 2002), which divides each brain hemisphere into 45 regions. For both atlases, we used a version in MNI-space that was then warped into subject-specific native space using FNIRT. Across both atlases, the edges of the network were derived from streamlines

that started and ended between the region pair and excluded streamlines that passed through one or both of the regions.

Weighted connectivity matrices were then generated from the atlases and DTI reconstructions such that the matrix **W** contained elements W_{ij} whose values were equal to the number of streamlines with end-to-end connectivity between regions i and j. All diagonal elements in the matrix were set to 0 to eliminate self-connections. To correct for differing region sizes, each matrix element was divided by the sum of the volumes of regions i and j (Hagmann et al. 2008). That is, $B_{ij} = W_{ij}/(v_{is}, +, v_{js})$ where v_{is} is the number of voxels in region i for subject s. The resultant connectivity matrix for each subject and scan was then normalized to give a *connection strength* **A** such that $A_{ij} = B_{ij}/\sum_{i,j} B_{ij}$, ensuring that all scans had identical total connection strength.

Network Statistics

Based on the functional analysis of this data set (Bassett et al. 2015), we examined whether individual variability in structural connectivity among distributed regions of the motor and visual systems was correlated with learning rate (Mattar et al. 2015). For both of these systems, we calculated the mean connection strength within the system by averaging the weights of all edges connecting pairs of nodes within the system (see Table 2). We report our results both at the single-scan level as well as an average over the 4 scans of each subject. Results are consistent in the 2 cases.

To analyze the impact of indirect connectivity between motor and visual regions, we computed *walk strength*, a measure of the connection strength between 2 regions that accounts for indirect paths of varying walk lengths. Here, a walk is defined as a path from one point in the graph to another that may pass along the same edge more than once (Fig. 6A). Given a graph **G** and its adjacency matrix **A**, A^n provides the connection strength between all pairs of nodes when examining walks of length n (Estrada and Hatano 2007). For instance, streamlines directly connecting primary visual cortex to primary motor cortex would be a walk of length 1, whereas the combination of streamlines connecting primary motor cortex first to thalamus and then to primary visual cortex would be a walk of length 2. Note that the term "length" is used in a topological sense, where walks with more steps are considered to have longer length (Crofts and Higham 2009). We base our analysis on a similar metric, *communicability*, which is defined such that walks of all lengths contribute to network communication, but longer walks increasingly contribute less. For an unweighted graph, the network communicability is simply given as $\sum_{n=1}^{\infty} A^n/n!$ (Estrada and Hatano 2007). In a weighted graph, an additional normalization is needed to prevent highly connected nodes from unduly dominating the estimate (Crofts and Higham 2009). A typical solution is to divide all weights A_{ij} by $\sqrt{d_i d_j}$, where d_i is the degree of node i, given by $d_i = \sum_{k=1}^{\infty} A_{ik}$ (Higham et al. 2007). While communicability provides a single metric of communication between nodes, it does not provide information on the contributions of specific walk lengths. To address this limitation, we define the *walk strength* as the normalized strength of walks of length n, which is given as S^n, where $S = D^{-1/2}AD^{-1/2}$ and $D = \mathrm{diag}(d_i)$, or the matrix whose diagonal is given by the values d_i (Crofts and Higham 2008).

Table 2 Brain areas in motor and visual systems derived directly from functional neuroimaging studies of the same task (Bassett et al. 2015)

Motor	Visual
L,R Precentral gyrus	L,R Intracalcarine cortex
L,R Postcentral gyrus	L,R Cuneus cortex
L,R Superior parietal lobule	L,R Lingual gyrus
L,R Supramarginal gyrus, anterior	L,R Supercalcarine cortex
L,R Supplemental motor area	L,R Occipital pole
L, Parietal operculum cortex	
R, Supramarginal gyrus, posterior	

Statistical Testing

Analysis was performed in Python using a collection of freely available packages: Numpy/Scipy, Pandas, stastmodels, and Jupyter. Correlations reported throughout the paper are Pearson correlations at an α level of 0.05. Data were corrected for multiple comparisons using Bonferroni, False Discovery Rate (Benjamini and Hochberg 1995), and the form $p < 0.05/n$, where n is the number of comparisons.

Results

Visual Streamline Connectivity Correlates with Learning

Our general aim was to uncover the structural network correlates of individual differences in learning rate for a common visuomotor task (Wymbs and Grafton 2015). Because direct connections between motor and visual cortices are not present at this large scale, we separately consider connectivity within motor areas and within visual areas previously identified in a functional analysis of this data set (Mattar et al. 2015, Bassett et al. 2015) (see Table 2 and Fig. 1A, B). We explicitly test the fundamental hypothesis that individuals with greater mean structural connectivity in motor and visual cortices would show faster learning rates (κ; see Materials and Methods) than individuals with less connectivity. We observed a highly significant correlation between visual–visual streamlines and learning rate across all subjects (Pearson correlation coefficient $r = 0.50$, with corresponding one-tailed p value of $p = 0.0125$, significant after Bonferroni correction; Fig. 3A). In contrast, we observed no significant correlation between motor–motor streamlines and learning rate ($r = 0.07$, $p = 0.389$; Fig. 3B).

Within the subset of connections linking visual regions with one another, we expected that connection strength within a given hemisphere would be particularly relevant given that interhemispheric transfer of information is not as relevant in this task as it is in other tasks manipulating perceptual reference frames (Bernier and Grafton 2010) or narrow visual fields (Doron et al. 2012). Consistent with our hypothesis, we found that the observed correlation between the visual-to-visual connection strength and learning rate was largely driven by intrahemispheric streamlines (Pearson correlation coefficient $r = 0.68$, $p = 0.0005$; Fig. 3C), while no significant correlation was observed among interhemispheric connections ($r = 0.01$, $p = 0.512$; Fig. 3D).

We verified these same relationships in the AAL atlas (Fig. 3E–H). The structural connection strength among visual–visual region pairs accounts for individual variability in learning rate. It is again more pronounced in both overall visual ($r = 0.44$, $p = 0.027$) and intrahemispheric visual–visual connectivity ($r = 0.62$, $p = 0.0002$), while no significant correlation is observed either in motor–motor connectivity ($r = 0.03$, $p = 0.449$) or in interhemispheric visual connections ($r = 0.10$, $p = 0.666$).

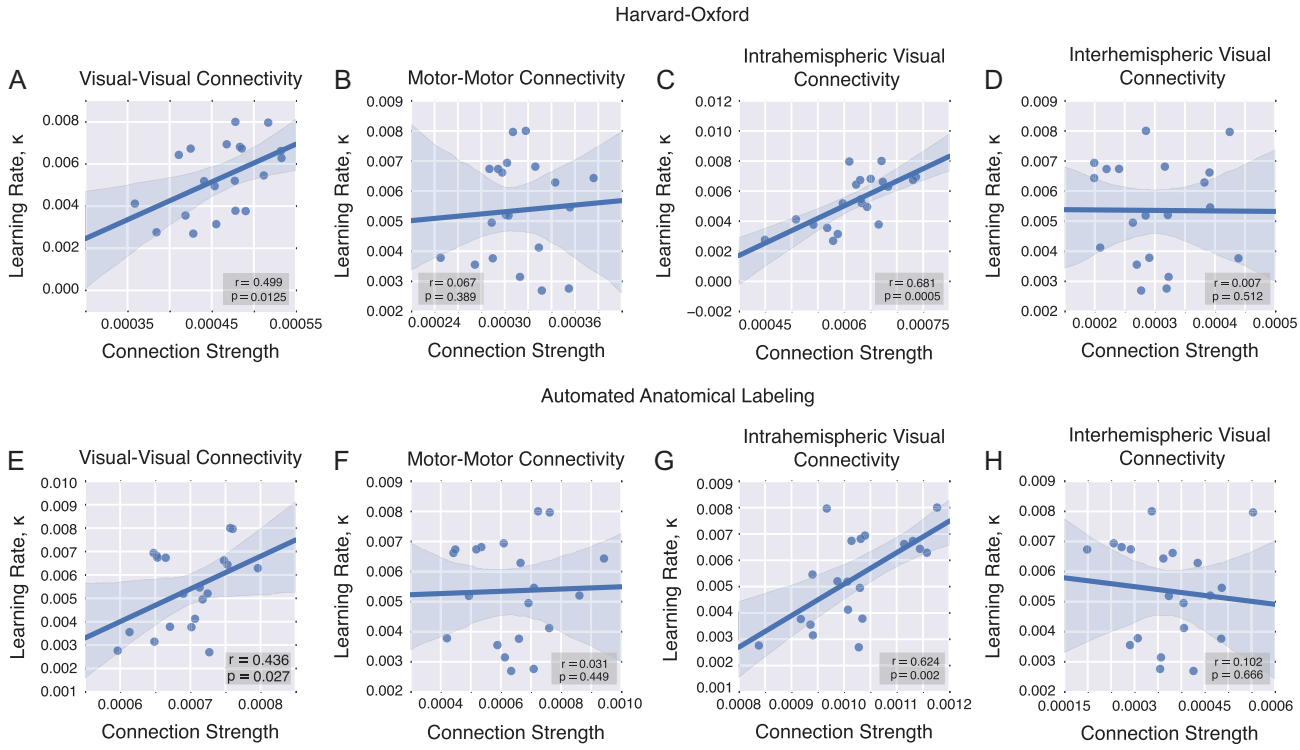

Figure 3. Correlations between mean connection strength and learning rate across all scanning sessions. (*A*) We observe a significant correlation between the average strength of connections linking visual regions and the learning rate. (*B*) No such relationship is observed for connections linking motor regions. The correlation between learning rate and visual–visual connectivity is largely driven by intrahemispheric (*C*) rather than interhemispheric (*D*) connections. (*E–H*) We observe the same relationships in the AAL atlas as in the Harvard-Oxford atlas for each subset of connections.

Reliability of Connectivity-Based Predictors of Learning

Next, we asked whether individual differences in the white matter connections that predicted learning rate would remain constant (Le Bihan and Johansen-Berg 2012) or change appreciably (Scholz et al. 2009, Blumenfeld-Katzir et al. 2011, Taubert et al. 2012) over 6 weeks of practice. We performed the same analysis as before but individually applied to each scan, restricting ourselves to the set of visual intrahemispheric connections (Fig. 4*A–D*). Across the 4 scan sessions, we observed a positive relationship between the visual-to-visual connection strength and learning rate: the p values for Scans 2–4 all pass a Bonferroni correction for $n = 4$ tests and Scan 1 was close to significant at $p = 0.05$. Pearson correlation coefficients and corresponding p values for Scan 1 were $r = 0.41$, $p = 0.050$, for Scan 2 were $r = 0.72$, $p = 0.0002$, for Scan 3 were $r = 0.61$, $p = 0.002$, and for Scan 4 were $r = 0.71$, $p = 0.0003$. These results suggest that the connectivity-learning relationship remained constant over 6 weeks of practice.

In addition to being robust across scanning sessions, the connectivity-learning relationship is also robustly observed when we segregated the brain into 90 (rather than 111) regions using a separate atlas. Specifically, using the AAL atlas, we observed a significant correlation between learning rate and intrahemispheric visual connection strength across all 4 scan sessions after Bonferroni correction for $n = 4$ tests (Fig. 4*E–H*). Pearson correlation coefficients and corresponding p values for Scan 1 were $r = 0.51$, $p = 0.011$, for Scan 2 were $r = 0.62$, $p = 0.002$, for Scan 3 were $r = 0.61$, $p = 0.002$, and for Scan 4 were $r = 0.54$, $p = 0.003$.

The scan-independent relationship between learning rate and visual-to-visual connectivity suggests the possibility that visual-to-visual connectivity itself is consistent across the 6 weeks of training, consistent with previous reports in other learning contexts (Le Bihan and Johansen-Berg 2012). To directly assess the reliability of visual-to-visual connectivity, we performed 2 separate analyses: first at the level of white matter streamlines and the second at the level of FA across voxels. First, we computed the intraclass correlation coefficient (ICC, Shrout and Fleiss 1979) to assess the reliability of visual connectivity across scanning sessions across the subset of subjects present for all 4 scans ($n = 17$). Using a 2-way ANOVA on visual-to-visual connection strength, we found no main effect of scanning session ($F_{3,48} = 1.35$, $p = 0.27$). Furthermore, the ICC is extremely high (ICC(1,1) = 0.83), which indicates the high reliability of visual-to-visual connection strength across scanning sessions. Additionally, we performed voxel-level univariate analyses to test for reliability of FA across the whole brain over the 6 weeks of learning. A repeated measures ANOVA was calculated across the 4 DTI scan sessions. An f-omnibus test demonstrated no significant effects ($p > 0.05$, FDR corrected). In addition, a paired t-test between Scans 1 and 4 was performed. There were no significant differences of FA values ($p > 0.05$, FDR corrected). These results support the conclusion that white matter microstructure remains consistent over the 4 scans, supporting the observed inter-scan reliability of our results.

Anatomical Specificity of Connectivity-Learning Relationship

To better understand the relationship between intrahemispheric visual connectivity and variability in learning rate κ, we examined which visual region pairs were driving this effect.

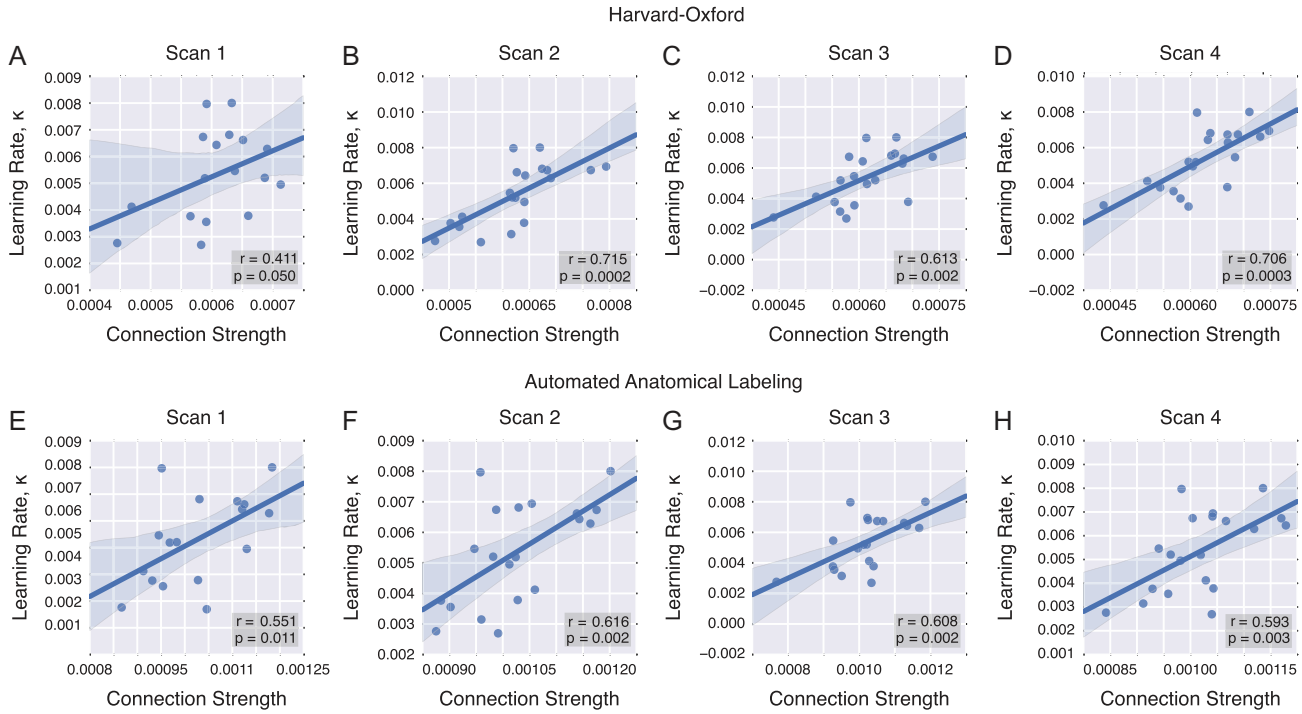

Figure 4. Connectivity-learning relationship by scan. (*A–D*) The structural connection strength between intrahemispheric visual–visual region pairs accounts for individual variability in learning rate, and this relationship is stable across the 4 scanning sessions. This relationship is significant after Bonferroni correction for Scans 2, 3, and 4 in the Harvard-Oxford atlas, with near significance in Scan 1. (*E–H*) We replicated these results within the AAL atlas, showing significance in all 4 scan sessions.

This examination had the added benefit of assessing whether different connections predicted behavior differently: although a positive trend was expected given the results in Figure 3, it is possible that a few smaller regions might show the opposite relationship. To address these questions, for each visual region pair, we calculated the Pearson correlation coefficient between the subject learning rate and the mean connection strength between the 2 regions across scans (see Fig. 5*A*). We found significant correlations (uncorrected) between learning rate and individual differences in the connections between 5 pairs of visual regions: right intracalcarine and right cuneal cortex $r = 0.64$, $p = 0.0012$), right cuneal cortex and right occipital pole $r = 0.42$, $p = 0.032$), left intracalcarine and left cuneal cortex $r = 0.56$, $p = 0.005$), left supracalcarine and left occipital cortex $r = 0.38$, $p = 0.049$), and left supracalcarine and left lingual gyrus $r = 0.4$, $p = 0.039$). Only the first of these relationships passed FDR correction for multiple comparisons (Fig. 5*B*).

Role of Indirect Connectivity in Learning Prediction

Our results have revealed structural correlates in direct connections *within* visual and motor regions; however, prior fMRI studies have linked changes in learning rate to functional connectivity *between* motor and visual areas (Bassett et al. 2015, Mattar et al. 2015). To examine structural predictors between regions, we turn to recently developed mathematical techniques in the domain of network science that allow us to directly examine the effects of indirect connectivity (an estimate of polysynaptic transmission potential across extended physical distances) in brain networks. Specifically, we compute variable walk lengths between any 2 nodes in a network. Direct connections are a walk length of 1, while connections that pass through one intermediary region have a walk length of 2; connections that pass through 2 intermediary regions have a walk length of 3, and so on (Fig. 6*A*). We hypothesized that as we examined sufficiently long walk lengths, the connectivity between motor and visual regions would become increasingly correlated with individual differences in learning rate.

Our results confirm this hypothesis, demonstrating that the length-specific connectivity between motor and visual regions was increasingly correlated with individual differences in learning rate as walk length increased. As shown in Figure 6, at walks of length 15, individual differences in walk strength between motor and visual regions were significantly correlated with individual differences in learning rate (Pearson correlation coefficient $r = 0.39$, $p = 0.004$). As walk length continued to increase, the correlation approached an asymptote which can be observed at $n = 40$ with $r = 0.56$, $p = 0.005$. We confirmed these assessments of statistical significance using a nonparametric null model wherein we shuffled node assignments to "visual" or "motor" sets, thereby choosing a random set of pseudo visual–motor edges. We examined the correlation at walks of $n = 40$ on repeated null model samples, and constructed a 95% threshold for the correlation coefficient from the null distribution. We observed that walks of length $n = 18$ and beyond all exceeded this threshold, and at $n = 40$ our data were significant compared with the null model at $p = 0.008$. These results indicate the importance of indirect connections between motor and visual cortices in facilitating the learning of a visuomotor task.

Discussion

In this study, we assess whether individual differences in structural connectivity can account for individual differences in learning a visuomotor task. Participants practiced a set of

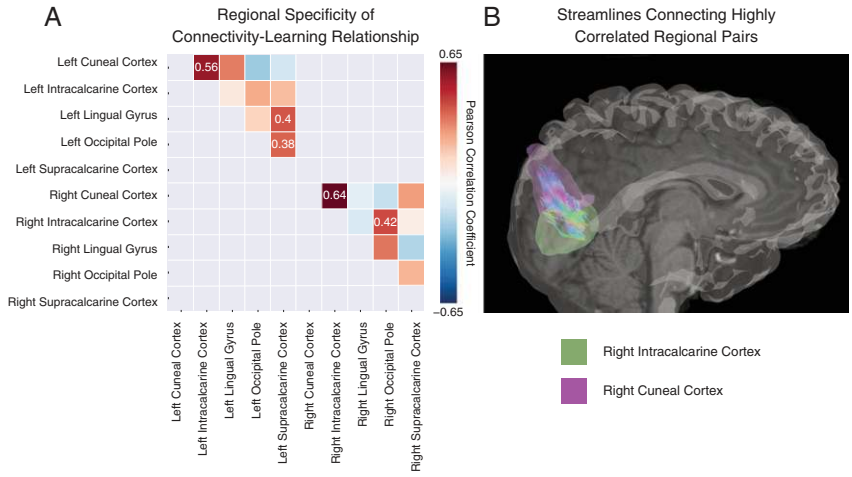

Figure 5. Anatomical specificity of visual-to-visual connection strength correlation with learning rate. (*A*) Significant correlation coefficients (uncorrected) between connection strength and learning rate κ for intrahemispheric visual regions are shown in colored boxes. We note relationships that pass a correction for multiple comparisons of the form $p < 0.05/n$, where n is the number of comparisons. Gray boxes were not included in the analysis, representing either duplicate entries or interhemisphere connections. (*B*) The reconstructed streamlines are shown for the only region pair that survives FDR correction: the connection between right intracalcarine cortex (green region) and right cuneal cortex (purple region).

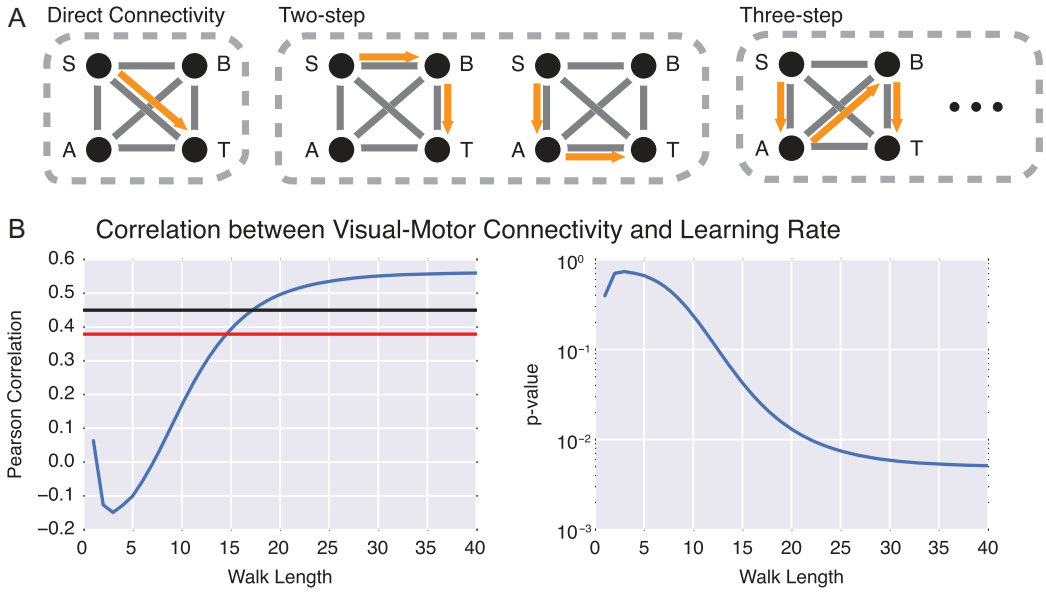

Figure 6. Indirect connections between visual and motor cortex facilitate learning. (*A*) Indirect connections between regions of interest can be quantified by walks on a structural network. Consider a toy graph in which paths exist from the source (*S*) to the target (*T*). The eventual flow of information between *S* and *T* will not only be influenced by direct connections, but also by indirect walks of length greater than one. (*B*) Correlation between individual differences in motor–visual connection strength at increasing walk lengths (measured by $(D^{-1/2}AD^{-1/2})^n$) and individual differences in learning rate κ. The correlation becomes significant at a walk length of $n = 15$. The red line indicates the $p = 0.05$ significance level calculated from the expectation of Pearson correlation coefficients in normal data; the black line indicates the $p = 0.05$ significance level calculated from a nonparametric permutation based null model in which node labels have been shuffled uniformly at random.

10-element sequences over a 6-week period, and we collected structural imaging data during 4 MRI scanning sessions spaced 2 weeks apart. We mapped structural connectivity between brain regions in large networks of interest in motor and visual systems, identified by prior assessments of functional neuroimaging data during task performance (Bassett et al. 2015). We observed a significant correlation between visual (but not motor) structural connectivity and learning rate across participants, and this relationship was consistent across the 4 scanning sessions. Interestingly, this correlation was strongest in direct connections among visual regions within the same hemisphere. However, an assessment of network walk strength also revealed a significant correlation between the strength of indirect connections *between* motor and visual cortices and individual differences in learning rate, suggesting the potential importance of physically extended polysynaptic information transmission for skill acquisition.

The relationship between white matter microstructure and human behavior: Our primary hypothesis posited that individual variability in white matter microstructure connecting task-relevant regions would account for individual differences in skill acquisition. Consistent with our hypothesis, we observed a significant relationship between intrahemispheric connections among visual region pairs and variability in learning rate on a

DSP task practiced over the course of 6 weeks. Previous studies have offered preliminary evidence to suggest that structural differences in specific brain regions (although not networks) correlate with individual differences in skill learning (Tuch et al. 2005, Tomassini et al. 2011). Our work extends these previous studies by demonstrating that the degree of connectivity within visual regions is correlated with individual differences in learning rate on a simple motor–visual task. While previous studies have focused on regional or tract-specific changes in FA in white matter, we demonstrate that tractography-based approaches capture individual differences in white matter that directly support skill acquisition. Of note, we do not observe longitudinal changes of FA in our study population over the course of training, suggesting that our diffusion measures of connectivity are remarkably stationary. Not surprisingly then, we found a remarkably consistent relationship between individual differences of connectivity and learning rate across all 4 DTI scanning sessions. While both tractography and FA-based approaches can reveal important structural differences, a tractography-based approach allows us to leverage network-based tools to understand brain- and system-wide dynamics.

Although we expected structural variability in both visual and motor systems would correlate with individual variability in learning rate, we only found a significant relationship with intrahemispheric connections among visual regions. We speculate that this may be due to the nature of the motor task itself. The participants learned to quickly press 1 of 5 buttons following a visual cue. This specific action (a button press) is not a particularly novel movement for these participants, all of whom have already developed a wide variety of dexterous skills such as typing. Due to the ubiquity of this action over the course of development, the structural connectivity within motor cortex may already be at a ceiling, obscuring any correlation with learning. Alternatively, it is possible that changes in motor connectivity with learning may only be measured at smaller spatial scales. In contrast to the simple button press, the more challenging skill that the subjects mastered was the spatial mapping between visual stimuli and motor commands. It is intuitively plausible that the ability to learn this mapping efficiently is fundamentally dependent on visual resources for detailed encoding of spatial information. Indeed, a wide range of visuomotor tasks have demonstrated strong reliance on occipital areas in mapping arbitrary stimuli with specific motor responses as well as sequences of responses (Grafton et al. 1994, 1995, Wiestler et al. 2014, Diedrichsen and Kornysheva 2015).

Structure is consistent across scanning sessions: Our results demonstrated a relationship between individual variability in learning rate and connection strength between visual regions that was consistent across the 4 scanning sessions. This consistency is particularly interesting in light of prior work showing changes in brain network connectivity as a function of experience-dependent plasticity (Pascual-Leone et al. 2005, Lindenberger et al. 2006). Indeed, researchers actively debate the time scales at which these structural changes occur (Holtmaat and Svoboda 2009, May 2011, Keller and Just 2015) and whether these changes can be detected using current diffusion weighted imaging techniques (Lövdén et al. 2013, Thomas and Baker 2013). Some of the most well-known experience-dependent plasticity changes have been reported from motor learning tasks (Zatorre et al. 2012). Using multiweek training paradigms in juggling, some of these studies have identified both volumetric changes in visual and parietal cortices (Scholz et al. 2009, Draganski et al. 2004) and FA changes in the posterior intraparietal sulcus (Scholz et al. 2009). Complementary work has examined structural correlates for professional piano players, identifying volumetric differences in motor and parietal regions (Gaser and Schlaug 2003) as well as structural connectivity differences in DTI data within the corticospinal tracts that connect motor cortex with the brainstem and spinal cord (Bengtsson et al. 2005). These training induced changes may arise from activity-dependent myelination (Fields 2015), which in turn may contribute to the observed changes in functional connectivity during long-term motor learning (Sampaio-Baptista et al. 2015). However, unlike juggling or extensive piano practice, our participants did not train on a complex visuomotor task, but instead, they learned a pairing between a visual cue and a required finger movement for a set of 6 sequences. In the context of this fine-motor training, we observed a stable relationship between visual connectivity and subject learning rate across all 4 scans, independent of the number of trials practiced.

A putative role for physically extended polysynaptic connections: Because prior work in functional neuroimaging has linked changes in learning rate to functional connectivity *between* motor and visual areas (Bassett et al. 2015, Mattar et al. 2015), we directly assessed indirect connectivity defined as a variant of network communicability that we called *walk strength*. This metric computes variable walk lengths where paths between 2 nodes can have increasing numbers of intermediary steps. For example, a 2-step walk could be taken from visual cortex through thalamus to motor cortex. We found that as walk length increased, individual differences in motor–visual connectivity were increasingly correlated with learning rate. These results suggest a role for physically extended sets of polysynaptic connections between motor and visual cortices that support the acquisition of this visuomotor skill. Such a role is consistent with previous work in computational neuroscience highlighting the role of highly structured circuits in sequence generation and memory (Hermundstad et al. 2011, Rajan et al. 2016). Indeed, in computational models at the neuron level, architectures reminiscent of chains (Levy et al. 2001, Fiete et al. 2010) and rings are particularly conducive to the generation of sequences. Our results complement these insights at small spatial scales to suggest that long-distance (chain-like) paths at the large scale of white matter tractography are supportive of sequence production. In future, it may be interesting to assess the generalizability of these results across other sequential learning tasks, and to determine the degree to which additional measurements of indirect connectivity (Goni et al. 2014) may differentially relate to learning rate, performance accuracy, and reaction time (Tuch et al. 2005).

Methodological Considerations

First, it is important to note that in this study, we rely on DTI and white matter tractography to estimate subject-specific and whole-brain structural connectivity. However, it is important to note that DTI-based tractographic reconstructions present a number of limitations. Among these is the tendency of current methods to present false positives and false negatives when compared with histological studies (Thomas et al. 2014, Reveley et al. 2015). However, diffusion imaging remains the only reliable method for studying human white matter structure noninvasively. Moreover, we expect potential tractography biases to be consistent across subjects, allowing us to accurately access individual differences in white matter architecture and its relationship to behavior. Second, it is also important to note that it

is not possible using these techniques to decipher the number of synapses present along the tracts between 2 regions, nor is it possible to decipher the number of synapses present along long-distance paths in the network. Thus, while data support a role for physically extended polysynaptic pathways, it do not directly speak to their microstructure. Third, it is important to note that while we hypothesized that interhemispheric connections would be less important for this task than for other tasks that require the manipulation of perceptual reference frames (Bernier and Grafton 2010) or that utilized a single visual hemifield (Doron et al. 2012), it is nevertheless possible that interhemispheric connections also play a role. It will be important in the future to implement higher resolution diffusion imaging to clarify the potential role of interhemispheric connections in the learning of this novel visuomotor skill. Fourth, it is interesting to ask whether the structural drivers of individual differences in learning rate are anatomically co-located with observed changes in functional connectivity during task performance. In fact, evidence suggests that this is not the case, and that instead regions that show individual differences in structural connectivity that are predictive of individual differences in learning rate are not the same as the regions that display changes in functional connectivity with training (Bassett et al. 2015). Together, these data suggest that further study is needed to understand the relationships between individual differences in structural connectivity and functional connectivity, and how they relate to gross changes in behavior or to individual differences in learning rate. Finally, we note that the lack of longitudinal changes in the strength of connectivity (measured both with FA and with the number of reconstructed streamlines between pairs of large-scale brain regions) could be explained either by neuroscientific or methodological factors. It is important to note that with this particular data set, we are unable to determine the origin of this consistency with complete confidence.

Conclusion

We identified variability in structural connectivity that accounts for individual differences in learning rate over 6 weeks of training on a visuomotor skill. Our analysis revealed direct connections among intrahemispheric visual regions as well as indirect connections between visual and motor cortices that suggest an underlying mechanism for differences in behavior. Clinically, these results offer novel biomarkers that may prove useful in predicting the time scales of motor rehabilitation following stroke and brain injury. In particular, because individuals with greater visual connectivity show swifter learning rates, a clinician may be able to predict the rate at which a patient will relearn a motor skill after a stroke based on the degree to which their visual system (and its indirect connections with the motor system) remain intact. More generally, our results may inform personalized training paradigms for healthy individuals; individuals with greater visual connectivity—and greater strength of indirect connectivity between motor and visual systems—may require less training to obtain the same proficiency as an individual with lesser connectivity and greater training. While speculative at this point, these possibilities motivate future work in clarifying the utility of white matter architecture in optimizing visuomotor training across healthy and injured populations.

Funding

D.S.B. and A.K. acknowledge support from the John D. and Catherine T. MacArthur Foundation, the Alfred P. Sloan Foundation, the Army Research Laboratory and the Army Research Office through contract numbers W911NF-10-2-0022 and W911NF-14-1-0679, the National Institute of Mental Health (2-R01-DC-009209-11), the National Institute of Child Health and Human Development (1R01HD086888-01), the Office of Naval Research, and the National Science Foundation (BCS-1441502, BCS-1430087, and PHY-1554488). S.T.G. and N.F.W. acknowledge support from the National Institute of Neurologic Disease and Stroke (1-P01-NS44393).

Notes

The content is solely the responsibility of the authors and does not necessarily represent the official views of any of the funding agencies. *Conflict of Interest Statement*: None declared.

References

1. Andersson JLR, Sotiropoulos SN. 2016. An integrated approach to correction for off-resonance effects and subject movement in diffusion MR imaging. NeuroImage. 125: 1063–1078.
2. Bassett DS, Brown JA, Deshpande V, Carlson JM, Grafton ST. 2011. Conserved and variable architecture of human white matter connectivity. Neuroimage. 54(2):1262–1279.
3. Bassett DS, Wymbs NF, Porter MA, Mucha PJ, Grafton ST. 2014. Cross-linked structure of network evolution. Chaos. 24(1):013112.
4. Bassett DS, Wymbs NF, Rombach MP, Porter MA, Mucha PJ, Grafton ST. 2013. Task-based core-periphery organization of human brain dynamics. PLoS Comput Biol. 9(9):e1003171.
5. Bassett DS, Yang M, Wymbs NF, Grafton ST. 2015. Learning-induced autonomy of sensorimotor systems. Nat Neurosci. 18(5):744–751.
6. Becker C, Pequito S, Pappas GJ, Miller MB, Grafton ST, Bassett DS, Preciado V. 2015. Accurately predicting functional connectivity from diffusion imaging. arXiv, 1512:02602.
7. Bengtsson SL, Nagy Z, Skare S, Forsman L, Forssberg H, Ullén F. 2005. Extensive piano practicing has regionally specific effects on white matter development. Nat Neurosci. 8 (9):1148–1150.
8. Benjamini Y, Hochberg Y. 1995. Controlling the false discovery rate: a practical and powerful approach to multiple testing. J R Stat Soc Series B.
9. Bernier PM, Grafton ST. 2010. Human posterior parietal cortex flexibly determines reference frames for reaching based on sensory context. Neuron. 68(4):776–788.
10. Betzel RF, Byrge L, He Y, Goni J, Zuo XN, Sporns O. 2014. Changes in structural and functional connectivity among resting-state networks across the human lifespan. Neuroimage. 102(Pt 2):345–357.
11. Blumenfeld-Katzir T, Pasternak O, Dagan M, Assaf Y. 2011. Diffusion MRI of structural brain plasticity induced by a learning and memory task. PLoS One. 6(6):e20678.
12. Cieslak M, Grafton ST. 2014. Local termination pattern analysis: a tool for comparing white matter morphology. Brain Imaging Behav. 8(2):292–299.
13. Crofts JJ, Higham DJ. 2008. Communicability in complex brain networks. arXiv.org.
14. Crofts JJ, Higham DJ. 2009. A weighted communicability measure applied to complex brain networks. J R Soc Interface. 6(33):411–414.

15. Crofts JJ, Higham DJ, Bosnell R, Jbabdi S, Matthews PM, Behrens TE, Johansen-Berg H. 2011. Network analysis detects changes in the contralesional hemisphere following stroke. Neuroimage. 54(1):161–169.
16. Crossman ERFW. 2010. A theory of the acquisition of speed-skill. Ergonomics. 2(2):153–166.
17. Dayan E, Cohen LG. 2011. Neuroplasticity subserving motor skill learning. Neuron. 72(3):443–454.
18. Diedrichsen J, Kornysheva K. 2015. Motor skill learning between selection and execution. Trends Cogn Sci. 19(4): 227–233.
19. Ding Y, Yao B, Lai Q, McAllister JP. 2001. Impaired motor learning and diffuse axonal damage in motor and visual systems of the rat following traumatic brain injury. Neurol Res. 23(2–3):193–202.
20. Doron KW, Bassett DS, Gazzaniga MS. 2012. Dynamic network structure of interhemispheric coordination. Proc Natl Acad Sci U S A. 109(46):18661–18668.
21. Draganski B, Gaser C, Busch V, Schuierer G, Bogdahn U, May A. 2004. Neuroplasticity: changes in grey matter induced by training. Nature. 427(6972):311–312.
22. Estrada E, Hatano N. 2007. Communicability in complex networks. 3:036111. arXiv.org.
23. Fields RD. 2015. A new mechanism of nervous system plasticity: activity-dependent myelination. Nat Rev Neurosci. 16 (12):756–767.
24. Fiete IR, Senn W, Wang CZ, Hahnloser RHR. 2010. Spike-time-dependent plasticity and heterosynaptic competition organize networks to produce long scale-free sequences of neural activity. Neuron. 65:563–576.
25. Gaser C, Schlaug G. 2003. Brain structures differ between musicians and non-musicians. J Neurosci: Official J Soc Neurosci. 23(27):9240–9245.
26. Goni J, van den Heuvel MP, Avena-Koenigsberger A, Velez de Mendizabal N, Betzel RF, Griffa A, Hagmann P, Corominas-Murtra B, Thiran JP, Sporns O. 2014. Resting-brain functional connectivity predicted by analytic measures of network communication. Proc Natl Acad Sci U S A. 111(2):833–838.
27. Grafton S, Hazeltine E, Ivry R. 1995. Functional mapping of sequence learning in normal humans. J Cogn Neurosci. 7(4): 497–510.
28. Grafton ST, Woods RP, Tyszka M. 1994. Functional imaging of procedural motor learning: relating cerebral blood flow with individual subject performance. Hum Brain Mapp. 1(3): 221–234.
29. Griffa A, Baumann PS, Thiran J-P, Hagmann P. 2013. Structural connectomics in brain diseases. NeuroImage. 80:515–526.
30. Hagmann P, Cammoun L, Gigandet X, Meuli R, Honey CJ, Wedeen VJ, Sporns O. 2008. Mapping the structural core of human cerebral cortex. PLoS Biol. 6(7):e159.
31. Heathcote A, Brown S, Mewhort DJ. 2000. The power law repealed: the case for an exponential law of practice. Psychon Bull Rev. 7(2):185–207.
32. Hermundstad AM, Bassett DS, Brown KS, Aminoff EM, Clewett D, Freeman S, Frithsen A, Johnson A, Tipper CM, Miller MB, et al. 2013. Structural foundations of resting-state and task-based functional connectivity in the human brain. Proc Natl Acad Sci U S A. 110(15):6169–6174.
33. Hermundstad AM, Brown KS, Bassett DS, Aminoff EM, Frithsen A, Johnson A, Tipper CM, Miller MB, Grafton ST, Carlson JM. 2014. Structurally-constrained relationships between cognitive states in the human brain. PLoS Comput Biol. 10(5):e1003591.
34. Hermundstad AM, Brown KS, Bassett DS, Carlson JM. 2011. Learning, memory, and the role of neural network architecture. PLoS Comput Biol. 7(6):e1002063.
35. Higham DJ, Kalna G, Kibble M. 2007. Spectral clustering and its use in bioinformatics. J Comput Appl Math. 204(1):25–37.
36. Hirsiger S, Koppelmans V, Merillat S, Liem F, Erdeniz B, Seidler RD, Jancke L. 2016. Structural and functional connectivity in healthy aging: associations for cognition and motor behavior. Hum Brain Mapp. 37(3):855–867.
37. Holtmaat A, Svoboda K. 2009. Experience-dependent structural synaptic plasticity in the mammalian brain. Nat Rev Neurosci. 10(9):647–658.
38. Honey CJ, Sporns O, Cammoun L, Gigandet X, Thiran JP, Meuli R, Hagmann P. 2009. Predicting human resting-state functional connectivity from structural connectivity. Proc Natl Acad Sci U S A. 106(6):2035–2040.
39. Hong SB, Zalesky A, Park S, Yang YH, Park MH, Kim B, Song IC, Sohn CH, Shin MS, Kim BN, et al. 2015. COMT genotype affects brain white matter pathways in attention-deficit/hyperactivity disorder. Hum Brain Mapp. 36(1):367–377.
40. Ingalhalikar M, Smith A, Parker D, Satterthwaite TD, Elliott MA, Ruparel K, Hakonarson H, Gur RE, Gur RC, Verma R. 2014. Sex differences in the structural connectome of the human brain. Proc Natl Acad Sci U S A. 111(2):823–828.
41. Jarbo K, Verstynen TD. 2015. Converging structural and functional connectivity of orbitofrontal, dorsolateral prefrontal, and posterior parietal cortex in the human striatum. J Neurosci: Official J Soc Neurosci. 35(9):3865–3878.
42. Jenkinson M, Bannister P, Brady M, Smith S. 2002. Improved optimization for the robust and accurate linear registration and motion correction of brain images. NeuroImage. 17(2): 825–841.
43. Jenkinson M, Beckmann CF, Behrens TEJ, Woolrich MW, Smith SM. 2012. FSL. NeuroImage. 62(2):782–790.
44. Jenkinson M, Smith S. 2001. A global optimisation method for robust affine registration of brain images. Med Image Anal. 5(2):143–156.
45. Jezzard P, Barnett AS, Pierpaoli C. 1998. Characterization of and correction for eddy current artifacts in echo planar diffusion imaging. Magn Reson Med. 39(5):801–812.
46. Johansen-Berg H. 2010. Behavioural relevance of variation in white matter microstructure. Curr Opin Neurol. 23(4): 351–358.
47. Keller TA, Just MA. 2015. Structural and functional neuroplasticity in human learning of spatial routes. NeuroImage. 125:256–266.
48. Le Bihan D, Johansen-Berg H. 2012. Diffusion MRI at 25: exploring brain tissue structure and function. NeuroImage. 61(2):324–341.
49. Leemans A, Jones DK. 2009. The B-matrix must be rotated when correcting for subject motion in DTI data. Magn Reson Med. 61(6):1336–1349.
50. Levy N, Horn D, Meilijson I, Ruppin E. 2001. Distributed synchrony in a cell assembly of spiking neurons. Neural Netw. 14:815–824.
51. Li Y, Liu Y, Li J, Qin W, Li K, Yu C, Jiang T. 2009. Brain anatomical network and intelligence. PLoS Comput Biol. 5(5): e1000395.
52. Lindenberger U, Li S-C, Bäckman L. 2006. Delineating brain-behavior mappings across the lifespan: substantive and methodological advances in developmental neuroscience. Neurosci Biobehav Rev. 30(6):713–717.
53. Lopez-Barroso D, Catani M, Ripolles P, Dell'Acqua F, Rodriguez-Fornells A, de Diego-Balaguer R. 2013. Word

learning is mediated by the left arcuate fasciculus. Proc Natl Acad Sci U S A. 110(32):13168–13173.
54. Lövdén M, Wenger E, Mårtensson J, Lindenberger U, Bäckman L. 2013. Structural brain plasticity in adult learning and development. Neurosci Biobehav Rev. 37(9 Pt B):2296–2310.
55. Lynch JC, Tian JR. 2006. Cortico-cortical networks and cortico-subcortical loops for the higher control of eye movements. Prog Brain Res. 151:461–501.
56. Mattar M, Wymbs NF, Bock A, Aguirre G, Grafton ST, Bassett DS. 2015. Predicting future learning from baseline network architecture. Submitted.
57. May A. 2011. Experience-dependent structural plasticity in the adult human brain. Trends Cogn Sci. 15(10):475–482.
58. Neumann N, Lotze M, Eickhoff SB. 2016. Cognitive expertise: an ale meta-analysis. Hum Brain Mapp. 37(1):262–272.
59. Newell A, Rosenbloom PS. 1993. Mechanisms of skill acquisition and the law of practice. MIT Press.
60. Osher DE, Saxe RR, Koldewyn K, Gabrieli JDE, Kanwisher N, Saygin ZM. 2016. Structural connectivity fingerprints predict cortical selectivity for multiple visual categories across cortex. Cerebral cortex (New York, N.Y. : 1991). 26(4):1668–1683.
61. Pascual-Leone A, Amedi A, Fregni F, Merabet LB. 2005. The plastic human brain cortex. Annu Rev Neurosci. 28(1): 377–401.
62. Rajan K, Harvey CD, Tank DW. 2016. Recurrent network models of sequence generation and memory. Neuron. 90(1): 128–142.
63. Reveley C, Seth AK, Pierpaoli C, Silva AC, Yu D, Saunders RC, Leopold DA, Ye FQ. 2015. Superficial white matter fiber systems impede detection of long-range cortical connections in diffusion MR tractography. Proc Natl Acad Sci U S A. 112(21):E2820–8.
64. Rhodes BJ, Bullock D, Verwey WB, Averbeck BB, Page MP. 2004. Learning and production of movement sequences: behavioral, neurophysiological, and modeling perspectives. Hum Mov Sci. 23(5):699–746.
65. Rosenbaum DA. 2014. Human Motor Control. Elsevier.
66. Sampaio-Baptista C, Filippini N, Stagg CJ, Near J, Scholz J, Johansen-Berg H. 2015. Changes in functional connectivity and GABA levels with long-term motor learning. Neuroimage. 106:15–20.
67. Sampaio-Baptista C, Khrapitchev AA, Foxley S, Schlagheck T, Scholz J, Jbabdi S, DeLuca GC, Miller KL, Taylor A, Thomas N, et al. 2013. Motor skill learning induces changes in white matter microstructure and myelination. J Neurosci. 33(50):19499–19503.
68. Scantlebury N, Cunningham T, Dockstader C, Laughlin S, Gaetz W, Rockel C, Dickson J, Mabbott D. 2014. Relations between white matter maturation and reaction time in childhood. J Int Neuropsychol Soc. 20(1):99–112.
69. Schmidt RA, Lee TD. 2005. Motor control and learning. In: A Behavioral Emphasis. Human Kinetics Publishers.
70. Scholz J, Klein MC, Behrens TE, Johansen-Berg H. 2009. Training induces changes in white-matter architecture. Nat Neurosci. 12(11):1370–1371.
71. Shrout PE, Fleiss JL. 1979. Intraclass correlations: uses in assessing rater reliability. Psychol Bull.
72. Smith SM. 2002. Fast robust automated brain extraction. Hum Brain Mapp. 17(3):143–155.
73. Smith SM, Fox PT, Miller KL, Glahn DC, Fox PM, Mackay CE, Filippini N, Watkins KE, Toro R, Laird AR, et al. 2009. Correspondence of the brain's functional architecture during activation and rest. Proc Natl Acad Sci U S A. 106(31): 13040–13045.
74. Smith SM, Jenkinson M, Woolrich MW, Beckmann CF, Behrens TEJ, Johansen-Berg H, Bannister PR, De Luca M, Drobnjak I, Flitney DE, et al. 2004. Advances in functional and structural MR image analysis and implementation as FSL. NeuroImage. 23:S208–S219.
75. Snoddy GS. 1926. Learning and stability: a psychophysiological analysis of a case of motor learning with clinical applications. J Appl Psychol. 10(1):1–36.
76. Sporns O, Tononi G, Kotter R. 2005. The human connectome: a structural description of the human brain. PLoS Comput Biol. 1(4):e42.
77. Taubert M, Villringer A, Ragert P. 2012. Learning-related gray and white matter changes in humans: an update. Neuroscientist. 18(4):320–325.
78. Thomas C, Baker CI. 2013. Teaching an adult brain new tricks: a critical review of evidence for training-dependent structural plasticity in humans. NeuroImage. 73:225–236.
79. Thomas C, Ye FQ, Irfanoglu MO, Modi P, Saleem KS, Leopold DA, Pierpaoli C. 2014. Anatomical accuracy of brain connections derived from diffusion MRI tractography is inherently limited. Proc Natl Acad Sci U S A. 111(46):16574–16579.
80. Tomassini V, Jbabdi S, Kincses ZT, Bosnell R, Douaud G, Pozzilli C, Matthews PM, Johansen-Berg H. 2011. Structural and functional bases for individual differences in motor learning. Hum Brain Mapp. 32(3):494–508.
81. Tuch DS, Salat DH, Wisco JJ, Zaleta AK, Hevelone ND, Rosas HD. 2005. Choice reaction time performance correlates with diffusion anisotropy in white matter pathways supporting visuospatial attention. Proc Natl Acad Sci. 102(34): 12212–12217.
82. Tunc B, Solmaz B, Parker D, Satterthwaite TD, Elliott MA, Calkins ME, Ruparel K, Gur RE, Gur RC, Verma R. 2016. Establishing a link between sex-related differences in the structural connectome and behaviour. Philos Trans R Soc Lond B Biol Sci. 371(1688).
83. Tzourio-Mazoyer N, Landeau B, Papathanassiou D, Crivello F, Etard O, Delcroix N, Mazoyer B, Joliot M. 2002. Automated anatomical labeling of activations in SPM using a macroscopic anatomical parcellation of the MNI MRI single-subject brain. NeuroImage. 15(1):273–289.
84. Wiestler T, Waters-Metenier S, Diedrichsen J. 2014. Effector-independent motor sequence representations exist in extrinsic and intrinsic reference frames. J Neurosci. 34(14): 5054–5064.
85. Wong FC, Chandrasekaran B, Garibaldi K, Wong PC. 2011. White matter anisotropy in the ventral language pathway predicts sound-to-word learning success. J Neurosci. 31(24): 8780–8785.
86. Wymbs NF, Grafton ST. 2015. The human motor system supports sequence-specific representations over multiple training-dependent timescales. Cerebral cortex (New York, N.Y. : 1991). 25(11):4213–4225.
87. Yarrow K, Brown P, Krakauer JW. 2009. Inside the brain of an elite athlete: the neural processes that support high achievement in sports. Nat Rev Neurosci. 10(8):585–596.
88. Yeh F-C, Verstynen TD, Wang Y, Fernández-Miranda JC, Tseng W-YI. 2013. Deterministic diffusion fiber tracking improved by quantitative anisotropy. PloS one. 8(11):e80713.
89. Yendiki A, Koldewyn K, Kakunoori S, Kanwisher N, Fischl B. 2013. Spurious group differences due to head motion in a diffusion MRI study. NeuroImage. 88C:79–90.
90. Zatorre RJ, Fields RD, Johansen-Berg H. 2012. Plasticity in gray and white: neuroimaging changes in brain structure during learning. Nature Publishing Group. 15(4):528–536.